# Deficiency in AMP-Activated Protein Kinase Exaggerates High Fat Diet-Induced Cardiac Hypertrophy and Contractile Dysfunction

**Subat Turdi**[1], **Machender R. Kandadi**[1], **Junxing Zhao**[2], **Anna F. Huff**[1], **Min Du**[2], and **Jun Ren**[1]

[1]Division of Pharmaceutical Sciences, Center for Cardiovascular Research and Alternative Medicine, University of Wyoming, Laramie, WY 82071, USA

[2]Department of Animal Sciences, Center for Cardiovascular Research and Alternative Medicine, University of Wyoming, Laramie, WY 82071, USA

## Abstract

AMPK, a metabolic sensor, protects against ischemic injury and cardiac hypertrophy although its role in obesity is unclear. This study was designed to examine the impact of AMPK deficiency on cardiac dysfunction following high fat feeding. Adult WT and transgenic mice overexpressing a kinase dead (KD) α2 isoform (K45R mutation) of AMPK were fed a low or high fat diet for 20 weeks. DEXA was used to confirm adiposity. Wheat germ agglutinin immunostaining was used to evaluate myocardial histology. Myocardial function was evaluated using echocardiography and edge-detection. AMPK activity was analyzed using fluorescence polarization assays. [1-$^{14}$C] oleate was used to determine fatty acid oxidation. Expression of AMPK, α1, α2, ACC, Akt, the Glut-4 translocation mediator Akt substrate of 160KD (AS160), mTOR, total and membrane Glut-4 was evaluated using Western blot. AMPK activity was decreased in KD mice regardless of diet regimen. High fat diet led to obesity, glucose intolerance and cardiac hypertrophy with accentuated glucose intolerance, dampened fatty acid oxidation and cardiac hypertrophy in KD mice. High fat feeding triggered lower fractional shortening, increased LV mass, left ventricular end diastolic/systolic diameter, decreased PS, $\pm$ dL/dt, prolonged TR$_{90}$ and intracellular Ca$^{2+}$ mishandling with a more pronounced effect in KD mice. High fat diet and AMPK KD lessened AMPKα2 isoform activity and ACC phosphorylation. AMPK deficiency unveiled or accentuated high fat diet-induced decrease in phosphorylation of Akt and AS160, membrane fraction of Glut-4 and mTOR expression (a greater mTOR phosphorylation). Taken together, these data suggest that AMPK deficiency exacerbates obesity-induced cardiac hypertrophy and contractile dysfunction, possibly associated with AS160 and mTOR signaling.

Correspondence to: Dr. Jun Ren Division of Pharmaceutical Sciences, Center for Cardiovascular Research and Alternative Medicine, University of Wyoming College of Health Sciences, Laramie, WY 82071, USA Tel: (307) 766-6131; Fax: (307) 766-2953 jren@uwyo.edu.

**Publisher's Disclaimer:** This is a PDF file of an unedited manuscript that has been accepted for publication. As a service to our customers we are providing this early version of the manuscript. The manuscript will undergo copyediting, typesetting, and review of the resulting proof before it is published in its final citable form. Please note that during the production process errors may be discovered which could affect the content, and all legal disclaimers that apply to the journal pertain.

DISCLOSURES
None.

**Keywords**

AMP-activated protein kinase; obesity; morphology; contraction

## INTRODUCTION

Obesity, if uncorrected, contributes to the onset and development of insulin resistance, cardiac hypertrophy, compromised myocardial contractile function, altered glucose, lipid and energy metabolism [1-3]. Although several theories have been postulated for obesity-induced cardiac morphological and functional anomalies including changes in cardiac fatty acid oxidation [4], increased myocardial oxygen consumption [5], oxidative stress [6], myocardial intracellular $Ca^{2+}$ handling [7], hyperleptinemia [2] and insulin resistance [8], the precise mechanism(s) of action responsible for obesity-induced cardiac disorders remains poorly understood. To better understand cardiac pathological changes in obesity, fat-enriched diet is used to foster the diet-induced pre-diabetic obesity [6]. Recent evidence from our laboratory as well as others has demonstrated insulin resistance, cardiac hypertrophy, myocardial dysfunction, downregulated mitochondrial oxidative phosphorylation and biogenesis in high fat diet-induced obesity [6;9;10]. Nonetheless, the pathogenesis of cardiac hypertrophy and contractile dysfunction following high fat diet intake still remains a mystery. Given that AMP-activated protein kinase (AMPK) has emerged as an important regulator of whole body energy metabolism with a close tie to diabetes mellitus and metabolic syndrome [11], increasing attention has been drawn towards the role of AMPK in energy expenditure and cardiovascular diseases. AMPK, which is highly expressed in the heart, is composed of a catalytic α-subunit, regulatory β- and γ-subunits. AMPK is activated via phosphorylation at $Thr^{172}$ by an increase in the cellular AMP/ATP ratio. Activated AMPK then switches on the energy producing processes while switching off the energy consuming processes [11]. Once activated, AMPK facilitates fatty acid oxidation by phosphorylating and thus inactivating acetyl-CoA carboxylase. In consequence, the inhibition of fatty acid uptake into mitochondria by malonyl-CoA, which inhibits carnitine palmitoyltransferase 1 (CPT-1), the rate limiting enzyme for mitochondrial uptake of long-chain carnitine acyl-CoAs [12]. In addition to fatty acid oxidation, AMPK may improve glucose metabolism *en route* to its cardioprotective property [13]. Activation of AMPK has been found to protect the heart against ischemic injury [14], reactive oxygen species-induced cell death [15] and pressure-overload-induced cardiac hypertrophy [16].

Although a role of AMPK signaling has been indicated in aging, obesity and insulin insensitivity [17-19], how defective AMPK signaling may contribute to cardiac dysfunction, insulin resistance and obesity is still unclear. Hence, we took advantage of a transgenic model with overexpression of a dominant-negative mutant α2 catalytic subunit of AMPK to examine the impact of AMPK deficiency on high fat diet-induced cardiac morphological and functional defects. Isoform-specific AMPK expression and activity were monitored. In an effort to elucidate the cellular mechanisms involved in AMPK deficiency and high fat-induced myocardial alterations, if any, special focus was made on AMPK and Akt, as well as their downstream target mammalian target of rapamycin (mTOR) and glycogen synthase kinase-3β (GSK-3β), which are pivotal in the maintenance of cell survival, glucose, lipid and energy metabolism in myocardium [20]. Since AMPK and Akt have been demonstrated to phosphorylate Akt substrate of 160KD (AS160) to initiate glucose transport by Glut-4 translocation to the plasma membrane [21;22], phosphorylation of AS160 and myocardial Glut-4 translocation were monitored in myocardium following high fat diet feeding in wild-type (WT) C57 and AMPK deficient mice.

## METHODS AND MATERIALS

### Experimental animals, diet feeding and intraperitoneal glucose tolerance test (IPGTT)

The experimental procedure was approved by our Institutional Animal Use and Care Committee and and was in compliance with the Guide for the Care and Use of Laboratory Animals published by the US National Institutes of Health (NIH Publication No. 85-23, revised 1996). In brief, 4 month-old male C57BL/6 and AMPK transgenic mice weighing ~20 g were randomly assigned to a low fat (10% of total calorie) or a high fat (45% of total calorie) diet (Research Diets Inc., New Brunswick, NJ) for 20 weeks. The AMPK transgenic mice overexpress a dominant negative α2 subunit of AMPK (kinase dead, KD, K45R mutation, KD1 line) driven by a muscle specific creatine kinase promoter to the skeletal and cardiac muscles were obtained from Dr. Morris Birnbaum (University of Pennsylvania, Philadelphia, PA) [23]. Littermates expressing wild-type of α2 subunit of AMPK were used as the control. Due to the replacement of functional α1, α2 and α3 isoforms by the KD α2 isoform, KD mice display very low AMPK activity in skeletal and cardiac muscles. AMPK KD mice were genotyped by PCR using the following primers: GGT CGA CGG TAT CGA TAA GCT TGA TAT C (forward) and GAA GGA ACC CGT TGG AGG ACT GGA GGC GAG G (reverse) [23]. Mice were housed in a climate-controlled environment (22.8 ± 2.0°C, 45-50% humidity) with a 12/12-light/dark cycle with free access to diet and water. After 5 months of feeding, body fat composition was measured using the Dual Energy X-ray Absorptiometry (DEXA, GE Lunar Prodigy™ 8743; Madison, WI). Difference in absorbance of the X-ray was detected based on tissue density. Percent fat was calculated using fat and body mass. Thereafter, mice were fasted for 12 hrs and were then given an intraperitoneal (i.p.) injection of glucose (2 g/kg b.w.). Blood samples were drawn from the tail vein immediately before the glucose challenge, as well as 15, 30, 60 and 120 min thereafter. Serum glucose levels were determined using an Accu-Chek III glucose analyzer. The area under the curve (AUC) was calculated using trapezoidal analysis for each adjacent time point and serum glucose level. Blood pressure was recorded using a CODA non-invasive blood pressure system (Kent Scientific Co, Torrington, CT) according to the instructions and were pooled from 3 readings from each mouse. Blood insulin levels were measured using an insulin enzyme-linked immunosorbent assay kit (Linco Research St. Charles, MO). In addition, left tibia of each animal was isolated at autopsy and tibial length was measured with a digital caliper.

### Echocardiography

Cardiac geometry and function were evaluated in anesthetized (Avertin 2.5%, 10 μl/g body wt i.p.) mice using a two-dimensional guided M-mode echocardiography (Sonos 5500, Phillips Medical System, Andover, MA) equipped with a 15–6 MHz linear transducer. Anterior and posterior wall thickness and diastolic and systolic left ventricular dimensions were recorded from M-mode images using the method adopted by the American Society of Echocardiography. Fractional shortening was calculated from end-diastolic diameter (EDD) and end-systolic diameter (ESD) using the following equation: (EDD -ESD)/EDD. Estimated echocardiographic left ventricular (LV) mass was calculated as [(LVEDD + septal wall thickness + posterior wall thickness) $^3$-LVEDD$^3$] *1.055, where 1.055 (mg/mm$^3$) is the density of myocardium. Heart rates were averaged over 10 cardiac cycles [24].

### Histological examination

Following anesthesia, hearts were arrested in diastole with saturated KCl, excised and fixed in 10% neutral-buffered formalin at room temperature for 24 hrs. The specimen was processed through graded alcohols, cleared in xylenes, embedded in paraffin, serial sections were cut at 5 μm. Deparaffinized slides were briefly rinsed with PBS and incubated in 0.1 mg/ml fluorescein isothiocyanate (FITC)-tagged wheat germ agglutinin ( FITC-WGA) for 2

hrs in the dark. Thereafter, the slides were washed with PBS 3 times, mounted with aqueous mounting media and coverslipped [25]. Cardiomyocyte cross-sectional areas were digitalized using an Olympus BX-51 microscope (Olympus America Inc., Melville, NY) equipped with a fluorescence filter and measured with the Image J (version1.44C) software [26].

## Isolation of cardiomyocytes

After ketamine/xylazine sedation, hearts were removed and perfused with Krebs-Henseleit bicarbonate (KHB) buffer containing (in mM): 118 NaCl, 4.7 KCl, 1.2 $MgSO_4$, 1.2 $KH_2PO_4$, 25 $NaHCO_3$, 10 HEPES and 11.1 glucose. Hearts were digested with collagenase D for 20 min. Left ventricles were removed and minced before being filtered. Myocyte yield was ~ 75% which was not affected by high fat diet or AMPK deficiency. Only rod-shaped myocytes with clear edges were selected for mechanical and intracellular $Ca^{2+}$ study [26].

## Cell shortening/relengthening

Mechanical properties of cardiomyocytes were assessed using an IonOptix$^{TM}$ soft-edge system (IonOptix, Milton, MA). Myocytes were placed in a chamber mounted on the stage of an Olympus IX-70 microscope and superfused (~2 ml/min at 25°C) with a KHB buffer containing 1 mM $CaCl_2$. Myocytes were field stimulated at 0.5 Hz unless otherwise stated. Cell shortening and relengthening were assessed including peak shortening (PS), time-to-PS (TPS), time-to-90% relengthening ($TR_{90}$) and maximal velocities of shortening/relengthening (± dL/dt) [26].

## Intracellular $Ca^{2+}$ transients

A cohort of myocytes was loaded with fura-2/AM (0.5 μM) for 10 min and fluorescence intensity were recorded witha a dual-excitation fluorescence photomultiplier system (Ionoptix, Milton, MA) Myocytes were placed onto an Olympus IX-70 inverted microscope and imaged through a Fluor × 40 oil objective. Cells were exposed to light emitted by a 75W lamp and passed through either a 360 or a 380 nm filter, while being stimulated to contract at 0.5 Hz. Fluorescence emissions were detected between 480-520 nm and qualitative change in fura-2 fluorescence intensity (FFI) was inferred from FFI ratio at the two wavelengths (360/380). Fluorescence decay time (both single and bi-exponential decay rates) was measured as an indication of intracellular $Ca^{2+}$ clearing rate [26].

## AMPK activity

Isoform-specific AMPK activity was measure on left ventricular lysate using an AMPK KinEASE™ FP Fluorescein Green Assay kit (Millipore, Bedford, MA) as described [19].

## Cardiac fatty acid oxidation

Cardiac fatty acid oxidation rate was determined in isolated cardiomyocytes with [1-$^{14}$C] oleate (Perkin-Elmer Life Sciences, Inc. Boston, MA) according to the previously described method with minor modifications [27-29]. In brief, cardiomyocytes were incubated in DMEM supplemented with [1-$^{14}$C] oleate (0.1 μCi/ml, 0.6 μM), 0.5% BSA, 1 mM L-carnitine, and 12.5 mM HEPES and maintained in a 24-well plate covered with parafilm for 1 hr under an atmosphere of 95% $O_2$/5% $CO_2$. The reactions were terminated by adding 100 μl of 70% perchloric acid and the released $^{14}CO_2$ was trapped in 200 μl of 1 M NaOH employing a fatty acid oxidation device described by Wang and colleagues [30]. To determine the oxidation rate, both $CO_2$ and $^{14}$C-acid-soluble products (ASMs) were calculated from the amount of $^{14}C(O_2)$ counted in Ecolite scintillation solution (ICN Biomedicals, Costa Mesa, CA) in a Beckman counter (LS5000 TD, Beckman Coulter,

Fullerton, CA). Results were expressed as picomole of substrate oxidized per hr per gram of protein (determined by the Bradford assay).

### Western blot analysis

Protein levels either total or phosphorylated Akt, AMPKα, ACC, AS160, GSK-3β, mTOR and Glut-4 were examined. The protein was prepared as described [6]. Samples containing equal amount of proteins were separated on 10% SDS-polyacrylamide gels in a minigel apparatus (Mini-PROTEAN II, Bio-Rad) and transferred to nitrocellulose membranes. The membranes were blocked with 5% milk in TBS-T, and were incubated overnight with anti-Akt (1:1,000), anti-pAkt (Ser473,1:1,000), anti-AMPKα (1:1,000), anti-pAMPK (Thr172, 1:1,000), anti-AMPKα2 (1:1,000), anti-AMPKα1 (1:1,000; Santa Cruz Biotechnology, Santa Cruz, CA), anti-ACC (Ser79, 1:1,000), anti-GSK-3β (1:1,000), anti-mTOR (1:1,000), anti-pmTOR (Ser2448, 1:1,000), anti-Glut4 (1:1,000) and anti-pAS160 (Thr642, 1:1,000; Upstate Biotechnology Lake Placid, NY). All antibodies above were purchased from Cell Signaling (Beverly, MA) unless otherwise indicated. Blots were then incubated for 1 hr with horseradish peroxidase (HRP)–conjugated secondary antibody (1:5,000). Antibody binding was detected using the enhanced chemiluminescence (Amersham Pharmacia, Piscataway, NJ). The film was scanned and the intensity of immunoblot bands was detected with a Bio-Rad Calibrated Densitometer (Model: GS-800). GAPDH and α-tubulin (Cell Signaling) were used as the loading controls.

### Myocardial membrane protein extraction

Cardiac muscle membrane protein was extracted using a membrane protein extraction kit (Biovision, Mountain View, CA). The membrane protein was subsequently used for Western blot analysis of Glut-4 [31].

### Statistical analysis

Data were expressed as Mean ± SEM. Statistical significance ($p < 0.05$) was estimated by one-way ANOVA followed by the Tukey's *post hoc* test. A two-way ANOVA with the Bonferroni correction was employed for the analysis of IPGTT.

## RESULTS

### General characteristics of experimental animals and IPGTT

Table 1 shows the general biometric characteristics of WT and AMPK KD mice fed low fat or high fat diet for 20 weeks. High fat feeding significantly increased body weight in WT and KD mice compared with the low fat-fed counterparts (by 28.6% and 26.8% in WT and KD mice, respectively). This is supported by the greater body fat composition depicting increased adiposity in high fat diet groups using DEXA scanning. High fat diet feeding increased heart weight and the heart weight-to-tibial length ratio in WT mice compared with WT-LF group, the effect of which was accentuated by AMPK deficiency. High fat feeding significantly increased liver and kidney weights but not the size of liver and kidney or blood pressure (diastolic and systolic) in a comparable manner in WT and AMPK KD groups. Fasting plasma insulin levels were equally elevated in WT and KD mice with the chronic high fat diet feeding. Following the intraperitoneal glucose challenge, serum glucose levels in low fat fed mice began to drop after peaking at 15 minand returned to baseline values after 120 min. Low fat-fed AMPK KD mice displayed slightly higher (although non-significant) serum glucose levels at 30 and 60 min compared with WT mice. However, the post-challenge glucose levels remained much higher in high fat-fed WT and KD mice, with a further increase in KD mice between 30 and 60 min. These data favor the presence of glucose intolerance following high fat diet feeding (Fig. 1A). This is consolidated by the

higher area underneath the curve (AUC) in both high fat groups with an exaggerated response in AMPK KD mice (Fig. 1B). These data indicate an exacerbated glucose disposal defect in AMPK KD mice following high fat feeding.

### Cardiac fatty acid oxidation

Data from $^{14}$C-oleate oxidation measurement revealed unaltered fatty acid oxidation in KD mice at basal level, consistent with an earlier report [14]. While high fat diet feeding exhibited a non-significant trend of decreased in oleate oxidation in WT mice, it significantly dampened fatty acid oxidation in AMPK KD mice (Fig. 1C).

### Effect of high fat feeding and AMPK deficiency on myocardial histology

To assess the impact of AMPK deficiency on myocardial histology following high fat diet feeding, cardiomyocyte cross-sectional area was examined. In FITC-WGA immunostained sections, high fat diet significantly increased the cardiomyocyte transverse cross-sectional area, consistent with the increased cardiac mass and size in WT and KD mice. Consistent with the gross biometric data (heart weight to tibial length ratio), the high fat diet-induced cardiomyocyte hypertrophy was significantly accentuated by AMPK deficiency (Fig. 2).

### Echocardiography

Twenty-weeks of high fat feeding significantly reduced left ventricular (LV) fractional shortening in WT mice compared to low fat fed controls, the effect of which was exaggerated by AMPK deficiency. LV wall thickness and heart rate were similar among all groups although high fat feeding triggered a marked increase in EDD and ESD compared with the low-fat fed mice. AMPK deficiency further accentuated the high fat diet-induced increase in EDD and ESD without eliciting any notable effect by itself. LV mass was significantly increased in high fat-fed mice with a further increase in high fat-fed KD mice. LV mass normalized to the murine body weight was equally enhanced in high fat diet-fed WT and KD mice without any effect of AMPK deficiency by itself (Table 1).

### Cardiomyocyte contractile and intracellular Ca$^{2+}$ properties

The resting myocyte length was comparable among in all groups. High fat diet feeding significantly decreased PS and $\pm$ dL/dt as well as prolonged TR$_{90}$ without affecting TPS in WT mice, the effects of which were exacerbated by AMPK deficiency (Fig. 3). Furthermore, high fat feeding significantly increased baseline intracellular Ca$^{2+}$ levels, depressed intracellular Ca$^{2+}$ rise in response to electrical stimulus ( FFI) and prolonged intracellular Ca$^{2+}$ decay time (single and bi-exponential fit) compared with the low fat feeding groups. AMPK deficiency exaggerated the prolonged single exponential intracellular Ca$^{2+}$ decay with subtle effect on high fat diet-elicited response in baseline intracellular Ca$^{2+}$, ΔFFI and bi-exponential intracellular Ca$^{2+}$ decay (Fig. 4).

### Effect of AMPK deficiency and high fat diet on AMPK α isoform expression and activity

Consistent with the previous studies [14;23], AMPKα2 isoform displayed slower protein migration in AMPK KD mice due to the c-myc–tag (Fig. 5A). AMPKα2 protein expression was comparable in WT and AMPK KD mice regardless of the fat content in diet although AMPKα2 isoform mutation led to a significant decrease in the expression of AMPK α1, again in line with the previous reports [14;23]. The isoform-specific AMPK activity assay revealed comparable AMPKα1 activity between WT and KD mice regardless of diet feeding regimen. Interestingly, AMPKα2 activity was significantly lower in low fat-fed KD mice compared with WT controls, validating the AMPK deficiency model as reported previously [14;23]. High fat feeding resulted in a significant decrease in AMPKα2 activity in WT mice with little further decline in KD mice (Fig. 5).

### Effect of AMPK deficiency and high fat diet on AMPK, pAMPK and pACC levels

Western blot analysis revealed that an upregulated total AMPK expression in both low fat and high fat diet-fed AMPK KD mice with a greater elevation in the KD-LF group. High fat diet feeding did not affect AMPK level in WT mice. Interestingly, AMPK phosphorylation, either in absolute value or pAMPK/AMPK ratio, was unaffected by either high fat diet or AMPK KD. Phosphorylation of ACC, a downstream target for AMPK, was depressed by high fat diet feeding and AMPK deficiency, with an additive effect of the two (Fig. 6).

### Effect of AMPK deficiency and high fat diet on Akt, AS160, Glut-4, GSK-3β and mTOR levels

To explore the possible mechanism of action behind AMPK deficiency- and high fat diet-induced cardiac morphological and functional alterations, expression and phosphorylation of Akt, AS160, Glut-4 (total and membrane-bound) and hypertrophic signaling (GSK-3β and mTOR) were examined in low fat and high fat diet-fed mice. Neither high fat diet nor AMPK deficiency affected Akt levels. Akt phosphorylation (absolute or pAkt/Akt ratio) was reduced in AMPK KD mice, regardless of the diet feeding regimen. Phosphorylation of AS160, which mediates glucose transport by Glut-4 translocation to the plasma membrane [21;22], was significantly depressed by the combined action of high fat diet and AMPK deficiency, but not either factor alone (Fig. 7). Although total Glut-4 expression was unchanged by high fat diet or AMPK deficiency, or both, high fat diet feeding significantly dampened the membrane fraction of Glut-4, the effect of which was accentuated by AMPK deficiency. Expression of the hypertrophic makers GSK-3β and phosphorylated mTOR was unaffected by either high fat diet or AMPK deficiency. However, combination of high fat diet and AMPK deficiency facilitated mTOR phosphorylation without affecting GSK-3β expression. Intriguingly, high fat diet feeding but not AMPK deficiency overtly downregulated mTOR expression with a greater decline in the AMPK KD mice. As a result, the pmTOR-to-mTOR ratio was significantly increased in the high fat diet-fed groups with a more pronounced rise in KD mice. AMPK deficiency itself failed to alter the pmTOR-tomTOR ratio in the absence of high fat diet feeding (Fig. 8).

## DISCUSSION

The major findings of our current study indicate that high fat diet feeding-induced obesity leads to glucose intolerance, hyperinsulinemia, cardiac hypertrophy, myocardial contractile dysfunction, and impaired intracellular $Ca^{2+}$ handling, the effects of which, with the exception of hyperinsulinemia, were exacerbated by the muscle-specific AMPK deficiency. Our results further revealed that AMPK KD mutation reduced AMPK activity, aggravated or unveiled the reduced phosphorylation of ACC and Akt or enhanced phosphorylation of mTOR following high fat diet feeding. These data are coincided with depressed AS160 phosphorylation and Glut-4 translocation in AMPK KD mice. AMPK deficiency exaggerated high fat diet-induced changes in cardiac hypertrophy and contractile dysfunction, in the absence of any innate harmful effect by AMPK deficiency itself, indicating an essential role of intact AMPK signaling in the cardiac hypertrophic changes and myocardial contractile dysfunction under diet-induced obesity.

Obesity-induced metabolic anomalies such as hypertension, insulin resistance, type 2 diabetes and dyslipidemia often elicit devastating health consequences [32]. Our present study revealed glucose intolerance, hyperinsulinemia, cardiac morphological and contractile defects following high fat feeding, consistent with the previous reports in both human and experimental models of obesity [1;3;6;8;9]. However, our 20-week high fat diet feeding regimen initiated obesity, glucose intolerance and hyperinsulinemia with little changes in blood pressure and fasting blood glucose, not favoring a major role of concomitant

hypertension and diabetes. The impaired intracellular $Ca^{2+}$ handling shown as decreased intracellular $Ca^{2+}$ release upon electrical stimulation and reduced intracellular $Ca^{2+}$ clearance rate in high fat diet-fed WT myocytes are in line with data from rodent models of high fat-induced obesity [6;9] and is likely responsible for prolonged relaxation, reduced peak shortening and maximal velocity of relengthening in high fat diet-fed mouse hearts. While the muscle specific AMPK deficiency itself did not affect body weight, heart weight and cardiomyocyte cross-sectional area, KD mice displayed dramatically enhanced cardiac hypertrophy without affecting whole body weight. Although AMPK deficiency itself failed to affect cardiomyocyte contractile and intracellular $Ca^{2+}$ properties, it significantly augmented obesity-elicited cardiomyocyte mechanical abnormalities. In particular, cardiomyocyte mechanical anomalies such as depressed peak shortening and maximal velocity of shortening/relengthening associated with prolonged duration of relaxation and intracellular $Ca^{2+}$ decay were accentuated in high fat-fed KD mice. Our study also revealed that cardiomyocytes from high fat-fed mice displayed reduced intracellular $Ca^{2+}$ rise in response to electrical stimulus and slowed intracellular $Ca^{2+}$ decay, indicating a predominant role of $Ca^{2+}$ resequestration (likely by SERCA) in the disrupted intracellular $Ca^{2+}$ homeostasis. It worth mentioning that AMPK deficiency itself did not overtly affect myocardial morphology, cardiomyocyte contractile and intracellular $Ca^{2+}$ properties in low fat diet group, suggesting that deficiency of this cellular fuel sensor is not innately harmful to the basal cardiac morphology and mechanical function. This is consistent with an earlier report using a somewhat similar AMPKα2 knockout mouse model [16]. Deficiency of AMPK, however, seems to have an overt detrimental influence on the heart under certain stress conditions such as pressure overload and advanced aging [16;19].

The heart as an energy-consuming organ mandates a constant supply of fuel and oxygen to maintain the intracellular ATP level and uninterrupted myocardial contraction/relaxation cycle [33]. Given that ~ 50 - 70% of total cardiac energy supply is derived from fatty acids, regulation of fatty acid oxidation by AMPK is crucial for normal cardiac function [14]. Our data showed that fatty acid oxidation and glucose disposal was severely impaired by high fat diet feeding in KD mice compared with WT mice. This finding is in line with an earlier study where ablation of AMPKα2 activity in skeletal muscle exacerbated insulin resistance induced by a 30-week high fat feeding [34]. As the predominant AMPK catalytic subunit in the heart [35], AMPKα2 plays a crucial role in the development of glucose intolerance and insulin resistance in skeletal muscles and adipose tissues [34;36]. In contrast, using the same mouse strain and similar high fat diet regimen, a recent study failed to reveal any AMPK-dependent effects on skeletal muscle glucose metabolism with high fat feeding [37]. Several factors may attribute to the discrepant findings between the earlier study and our current work such as the duration of high fat feeding (12 versus 20 weeks), the age of the mice at the start of fat feeding (6-9 weeks versus 16 weeks), difference in tissues (skeletal muscle versus cardiac muscle) and different modes of substrate preference and metabolism under high fat diet setting. It is also important to point out that the KD mice used in both studies [37] elicits higher levels of mutant α2 expression in skeletal over cardiac muscles [23]. Nonetheless, AMPKα2 activity is reduced remarkably in cardiac muscles similar to skeletal muscles [14].

Our data revealed an elevated AMPKα protein expression (reflecting overexpression of mutant α2 subunit) associated with unchanged AMPK phosphorylation in AMPK KD mice, consistent with the report of unchanged AMPKα phosphorylation in skeletal muscles of AMPK KD mice [23]. Our observation revealed significantly depressed AMPKα2 isoform activity and phosphorylation of ACC, an AMPK downstream signaling molecule, in AMPK KD mice, validating the AMPK KD transgenic model. It has been demonstrated that high fat diet or obesity is associated with a reduced AMPK activity [38]. In our hand, high fat diet significantly decreased pACC in the absence of notable change in pAMPK, prompting a

high fat diet-induced inhibitory effect on AMPK activity with little role of the AMPK upstream activators such as LKB1. AMPK was shown to regulate intracellular fatty acid oxidation via inactivating ACC [39]. The reduced pACC levels in diet-induced obesity suggest a pivotal role of AMPK in obesity-triggered inefficient fatty acid oxidation and insulin resistance. In agreement with a previous report [14], oleate oxidation in KD mice did not change with low fat diet feeding, suggesting basal fatty acid oxidation was less likely to be affected by AMPK deficiency (supported by our data). Given the observation of the overtly reduced ACC phosphorylation in high fat diet-fed KD mice, our finding of reduced fatty acid oxidation in these same mice may stem from decreased CPT-1 activity. However, upstream AMPK kinases, glucose oxidation, fatty acid transporters and hepatic glucose production warrant further scrutiny in the face of the impaired fatty acid oxidation and glucose disposal in KD mice following high fat diet feeding. In addition, while the ACC phosphorylation pathway is beyond the scope of our study, further research should be focused on the role of ACC phosphorylation and fatty acid transport/uptake (e.g., due to a higher level of malonyl-CoA) in obesity-induced cardiovascular complications.

Several mechanisms may be considered for the AMPK KD-elicited exaggeration of high fat diet-induced morphological, mechanical and intracellular $Ca^{2+}$ dysregulation. First, our data suggest that AMPK deficiency may promote high fat diet-induced mTOR phosphorylation (resulted from downregulated mTOR expression). Inhibition of AMPK is known to stimulate mTOR signaling [40]. Enhanced mTOR phosphorylation directly promotes cardiac hypertrophy [41;42], interrupt cardiac contractile function and intracellular $Ca^{2+}$ homeostasis [43]. Second, AMPK deficiency was found to unveil a reduced AS160 phosphorylation following high fat diet feeding. This is supported by the overtly downregulated Glut-4 translocation in high fat-fed KD mice, indicating a poor Glut-4 mediated glucose disposal in the presence of AMPK deficiency and high fat diet feeding. In our study, a reduction in Glut-4 expression was observed in high fat diet-fed WT mice, which is supported by previous findings [44-46]. It is well accepted that intact insulin sensitivity through Glut-4 translocation is essential to the maintenance of cardiac contractile function [47]. Our study further revealed depressed Akt phosphorylation in KD mice, depicting a role of Akt in AMPK deficiency-associated exaggeration of myocardial response in obesity. AS160 is a downstream target for both Akt [48] and AMPK [49]. Therefore, reduced AS160 phosphorylation may likely be responsible for the impaired Glut-4 translocation in high fat-fed KD mice. Last but not least, decreased fatty acid oxidation may also contribute to the impairment in substrate utilization. It is well accepted that excess lipid accumulation in the heart leads to cardiac lipotoxicity and contractile dysfunction [50].

In summary, our findings suggest that maintenance of AMPK signaling may be essential in the preservation of ventricular function in obesity. These data favor the notion that AMPK may serve as a potential therapeutic target for obesity and obesity-associated complications. Although our present study has shed some light on the role of Akt, mTOR and AS160 in high fat diet-induced myocardial defects, the pathogenesis of cardiac morphological and contractile dysfunction in obesity still deserves further in-depth investigation. As the obesity epidemic continues to rise worldwide, cardiac implication of obesity is becoming a more pertinent health care issue. A better and thorough understanding of the genetic and environmental maneuvers of energy metabolism in obesity should help to ramify not only obesity but also obesity-associated cardiovascular anomalies.

## Acknowledgments

## Reference List

1. Eckel RH, Barouch WW, Ershow AG. Report of the National Heart, Lung, and Blood Institute-National Institute of Diabetes and Digestive and Kidney Diseases Working Group on the pathophysiology of obesity-associated cardiovascular disease. Circulation 2002;105:2923–8. [PubMed: 12070124]

2. Ren J, Ma H. Impaired cardiac function in leptin-deficient mice. Curr Hypertens Rep 2008;10:448–53. [PubMed: 18959830]

3. Sowers JR. Obesity as a cardiovascular risk factor. Am J Med 2003;115(Suppl 8A):37S–41S. [PubMed: 14678864]

4. Feuvray D, Darmellah A. Diabetes-related metabolic perturbations in cardiac myocyte. Diabetes Metab 2008;34(Suppl 1):S3–S9. [PubMed: 18358420]

5. Boudina S, Abel ED. Mitochondrial uncoupling: a key contributor to reduced cardiac efficiency in diabetes. Physiology (Bethesda) 2006;21:250–8. [PubMed: 16868314]

6. Dong F, Li Q, Sreejayan N, et al. Metallothionein prevents high-fat diet induced cardiac contractile dysfunction: role of peroxisome proliferator activated receptor gamma coactivator 1alpha and mitochondrial biogenesis. Diabetes 2007;56:2201–12. [PubMed: 17575086]

7. Lima-Leopoldo AP, Sugizaki MM, Leopoldo AS, et al. Obesity induces upregulation of genes involved in myocardial Ca2+ handling. Braz J Med Biol Res 2008;41:615–20. [PubMed: 18719744]

8. Ouwens DM, Boer C, Fodor M, et al. Cardiac dysfunction induced by high-fat diet is associated with altered myocardial insulin signalling in rats. Diabetologia 2005;48:1229–37. [PubMed: 15864533]

9. Relling DP, Esberg LB, Fang CX, et al. High-fat diet-induced juvenile obesity leads to cardiomyocyte dysfunction and upregulation of Foxo3a transcription factor independent of lipotoxicity and apoptosis. J Hypertens 2006;24:549–61. [PubMed: 16467659]

10. Sparks LM, Xie H, Koza RA, et al. A high-fat diet coordinately downregulates genes required for mitochondrial oxidative phosphorylation in skeletal muscle. Diabetes 2005;54:1926–33. [PubMed: 15983191]

11. Hardie DG. AMPK: a key regulator of energy balance in the single cell and the whole organism. Int J Obes (Lond) 2008;32(Suppl 4):S7–12. [PubMed: 18719601]

12. Merrill GF, Kurth EJ, Hardie DG, Winder WW. AICA riboside increases AMP-activated protein kinase, fatty acid oxidation, and glucose uptake in rat muscle. Am J Physiol 1997;273:E1107–E1112. [PubMed: 9435525]

13. Hardie DG. AMP-activated protein kinase: the guardian of cardiac energy status. J Clin Invest 2004;114:465–8. [PubMed: 15314681]

14. Russell RR III, Li J, Coven DL, et al. AMP-activated protein kinase mediates ischemic glucose uptake and prevents postischemic cardiac dysfunction, apoptosis, and injury. J Clin Invest 2004;114:495–503. [PubMed: 15314686]

15. Hwang JT, Kwon DY, Park OJ, Kim MS. Resveratrol protects ROS-induced cell death by activating AMPK in H9c2 cardiac muscle cells. Genes Nutr 2008;2:323–6. [PubMed: 18850225]

16. Zhang P, Hu X, Xu X, et al. AMP activated protein kinase-alpha2 deficiency exacerbates pressure-overload-induced left ventricular hypertrophy and dysfunction in mice. Hypertension 2008;52:918–24. [PubMed: 18838626]

17. Steinberg GR, Jorgensen SB. The AMP-activated protein kinase: role in regulation of skeletal muscle metabolism and insulin sensitivity. Mini Rev Med Chem 2007;7:519–26. [PubMed: 17504187]

18. Viollet B, Andreelli F, Jorgensen SB, et al. The AMP-activated protein kinase alpha2 catalytic subunit controls whole-body insulin sensitivity. J Clin Invest 2003;111:91–8. [PubMed: 12511592]

19. Turdi S, Fan X, Li J, et al. AMP-activated protein kinase deficiency exacerbates aging-induced myocardial contractile dysfunction. Aging Cell 2010;9:592–606. [PubMed: 20477759]

20. Oudit GY, Sun H, Kerfant BG, et al. The role of phosphoinositide-3 kinase and PTEN in cardiovascular physiology and disease. J Mol Cell Cardiol 2004;37:449–71. [PubMed: 15276015]

21. Funai K, Cartee GD. Inhibition of contraction-stimulated AMP-activated protein kinase inhibits contraction-stimulated increases in PAS-TBC1D1 and glucose transport without altering PAS-AS160 in rat skeletal muscle. Diabetes 2009;58:1096–104. [PubMed: 19208911]

22. Chavez JA, Roach WG, Keller SR, et al. Inhibition of GLUT4 translocation by Tbc1d1, a Rab GTPase-activating protein abundant in skeletal muscle, is partially relieved by AMP-activated protein kinase activation. J Biol Chem 2008;283:9187–95. [PubMed: 18258599]

23. Mu J, Brozinick JT Jr. Valladares O, et al. A role for AMP-activated protein kinase in contraction- and hypoxia-regulated glucose transport in skeletal muscle. Mol Cell 2001;7:1085–94. [PubMed: 11389854]

24. Gardin JM, Siri FM, Kitsis RN, et al. Echocardiographic assessment of left ventricular mass and systolic function in mice. Circ Res 1995;76:907–14. [PubMed: 7729009]

25. Wang D, Patel VV, Ricciotti E, et al. Cardiomyocyte cyclooxygenase-2 influences cardiac rhythm and function. Proceedings of the National Academy of Sciences 2009;106:7548–52.

26. Doser TA, Turdi S, Thomas DP, et al. Transgenic overexpression of aldehyde dehydrogenase-2 rescues chronic alcohol intake-induced myocardial hypertrophy and contractile dysfunction. Circulation 2009;119:1941–9. [PubMed: 19332462]

27. Barger PM, Brandt JM, Leone TC, et al. Deactivation of peroxisome proliferator-activated receptor-alpha during cardiac hypertrophic growth. J Clin Invest 2000;105:1723–30. [PubMed: 10862787]

28. Veerkamp JH, Van Moerkerk HT. The effect of malonyl-CoA on fatty acid oxidation in rat muscle and liver mitochondria. Biochim Biophys Acta 1982;710:252–5. [PubMed: 7066363]

29. Schaap FG, Binas B, Danneberg H, et al. Impaired long-chain fatty acid utilization by cardiac myocytes isolated from mice lacking the heart-type fatty acid binding protein gene. Circ Res 1999;85:329–37. [PubMed: 10455061]

30. Wang X, Wang R, Nemcek TA, et al. A self-contained 48-well fatty acid oxidation assay 1. Assay Drug Dev Technol 2004;2:63–9. [PubMed: 15090211]

31. Dong F, Kandadi MR, Ren J, Sreejayan N. Chromium (D-phenylalanine)3 supplementation alters glucose disposal, insulin signaling, and glucose transporter-4 membrane translocation in insulin-resistant mice. J Nutr 2008;138:1846–51. [PubMed: 18806091]

32. Cannon CP. Obesity-related cardiometabolic complications. Clin Cornerstone 2008;9:11–22. [PubMed: 19046736]

33. Bertrand L, Horman S, Beauloye C, Vanoverschelde JL. Insulin signalling in the heart. Cardiovasc Res 2008;79:238–48. [PubMed: 18390897]

34. Fujii N, Ho RC, Manabe Y, et al. Ablation of AMP-activated protein kinase alpha2 activity exacerbates insulin resistance induced by high-fat feeding of mice. Diabetes 2008;57:2958–66. [PubMed: 18728234]

35. Tian R, Musi N, D'Agostino J, et al. Increased adenosine monophosphate-activated protein kinase activity in rat hearts with pressure-overload hypertrophy. Circulation 2001;104:1664–9. [PubMed: 11581146]

36. Villena JA, Viollet B, Andreelli F, et al. Induced adiposity and adipocyte hypertrophy in mice lacking the AMP-activated protein kinase-alpha2 subunit. Diabetes 2004;53:2242–9. [PubMed: 15331533]

37. Beck JS, O'Neill HM, Hewitt K, et al. Reduced AMP-activated protein kinase activity in mouse skeletal muscle does not exacerbate the development of insulin resistance with obesity. Diabetologia 2009;52:2395–404. [PubMed: 19688337]

38. Liu Y, Wan Q, Guan Q, et al. High-fat diet feeding impairs both the expression and activity of AMPKa in rats' skeletal muscle. Biochem Biophys Res Commun 2006;339:701–7. [PubMed: 16316631]

39. Kudo N, Barr AJ, Barr RL, et al. High rates of fatty acid oxidation during reperfusion of ischemic hearts are associated with a decrease in malonyl-CoA levels due to an increase in 5'-AMP-activated protein kinase inhibition of acetyl-CoA carboxylase. J Biol Chem 1995;270:17513–20. [PubMed: 7615556]

40. Xue B, Kahn BB. AMPK integrates nutrient and hormonal signals to regulate food intake and energy balance through effects in the hypothalamus and peripheral tissues. J Physiol 2006;574:73–83. [PubMed: 16709629]

41. McMullen JR, Sherwood MC, Tarnavski O, et al. Inhibition of mTOR Signaling With Rapamycin Regresses Established Cardiac Hypertrophy Induced by Pressure Overload. Circulation 2004;109:3050–5. [PubMed: 15184287]

42. Dolinsky VW, Chan AYM, Robillard Frayne I, et al. Resveratrol Prevents the Prohypertrophic Effects of Oxidative Stress on LKB1. Circulation 2009;119:1643–52. [PubMed: 19289642]

43. Li SY, Fang CX, Aberle NS, et al. Inhibition of PI-3 kinase/Akt/mTOR, but not calcineurin signaling, reverses insulin-like growth factor I-induced protection against glucose toxicity in cardiomyocyte contractile function. J Endocrinol 2005;186:491–503. [PubMed: 16135669]

44. Pedersen O, Kahn CR, Flier JS, Kahn BB. High fat feeding causes insulin resistance and a marked decrease in the expression of glucose transporters (Glut 4) in fat cells of rats. Endocrinology 1991;129:771–7. [PubMed: 1855475]

45. Miura T, Suzuki W, Ishihara E, et al. Impairment of insulin-stimulated GLUT4 translocation in skeletal muscle and adipose tissue in the Tsumura Suzuki obese diabetic mouse: a new genetic animal model of type 2 diabetes. Eur J Endocrinol 2001;145:785–90. [PubMed: 11720905]

46. Wright JJ, Kim J, Buchanan J, et al. Mechanisms for increased myocardial fatty acid utilization following short-term high-fat feeding. Cardiovasc Res 2009;82:351–60. [PubMed: 19147655]

47. Tian R, Abel ED. Responses of GLUT4-deficient hearts to ischemia underscore the importance of glycolysis. Circulation 2001;103:2961–6. [PubMed: 11413087]

48. Sakamoto K, Holman GD. Emerging role for AS160/TBC1D4 and TBC1D1 in the regulation of GLUT4 traffic. Am J Physiol Endocrinol Metab 2008;295:E29–E37. [PubMed: 18477703]

49. Kramer HF, Witczak CA, Fujii N, et al. Distinct signals regulate AS160 phosphorylation in response to insulin, AICAR, and contraction in mouse skeletal muscle. Diabetes 2006;55:2067–76. [PubMed: 16804077]

50. Zhang Y, Ren J. Role of cardiac steatosis and lipotoxicity in obesity cardiomyopathy. Hypertension 2010;56 in press.
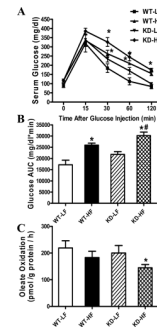
**Fig. 1.**
Intraperitoneal glucose tolerance test (IPGTT, 2 g/kg) in low fat (LF) or high fat (HF)-fed WT and AMPK KD mice. A: Serum glucose levels within 120 min following glucose challenge; B: Area underneath the curve (AUC). C: Oleate oxidation rate in isolated cardiomyocytes from LF- or HF-fed WT and AMPK KD mice. Mean ± SEM, n = 3-6 mice per group, * $p < 0.05$ *vs.* WT-LF group, # $p < 0.05$ *vs.* WT-HF group.
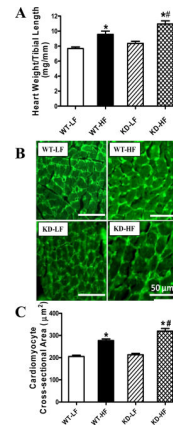
**Fig. 2.**
Analysis of cardiac hypertrophy in hearts from WT and AMPK KD mice with low fat (LF) or high fat (HF) diet intake. A: Normalization of heart weight to tibial length from LF- or HF-fed WT and AMPK KD mice; B: FITC-conjugated wheat germ agglutinin immunostaining depicting transverse sections of left ventricular myocardium from LF- or HF-fed WT and KD mice (magnification, ×400); C: Quantitative analysis of cardiomyocyte cross-sectional (transverse) area in ~ 200 cells from 4 - 5 mice per group, Mean ± SEM, n = 13-15 mice per group, * p < 0.05 *vs.* WT-LF group, # p < 0.05 *vs.* WT-HF group.
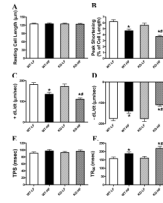
**Fig 3.**
Cardiomyocyte contractile properties from low fat (LF) and high fat (HF)-fed WT and
AMPK KD mouse hearts. A: Resting cell length (CL); B: Peak shortening (PS, normalized
to CL); C: Maximal velocity of shortening (+ dL/dt); D: Maximal velocity of relengthening
(-dL/dt); E: Time-to-PS (TPS); and F: Time-to-90% relengthening ($TR_{90}$). Mean ± SEM, n
= 85-86 cells per group from 3-4 mice, * $p < 0.05$ *vs.* WT-LF group, # $p < 0.05$ *vs.* WT-HF
group
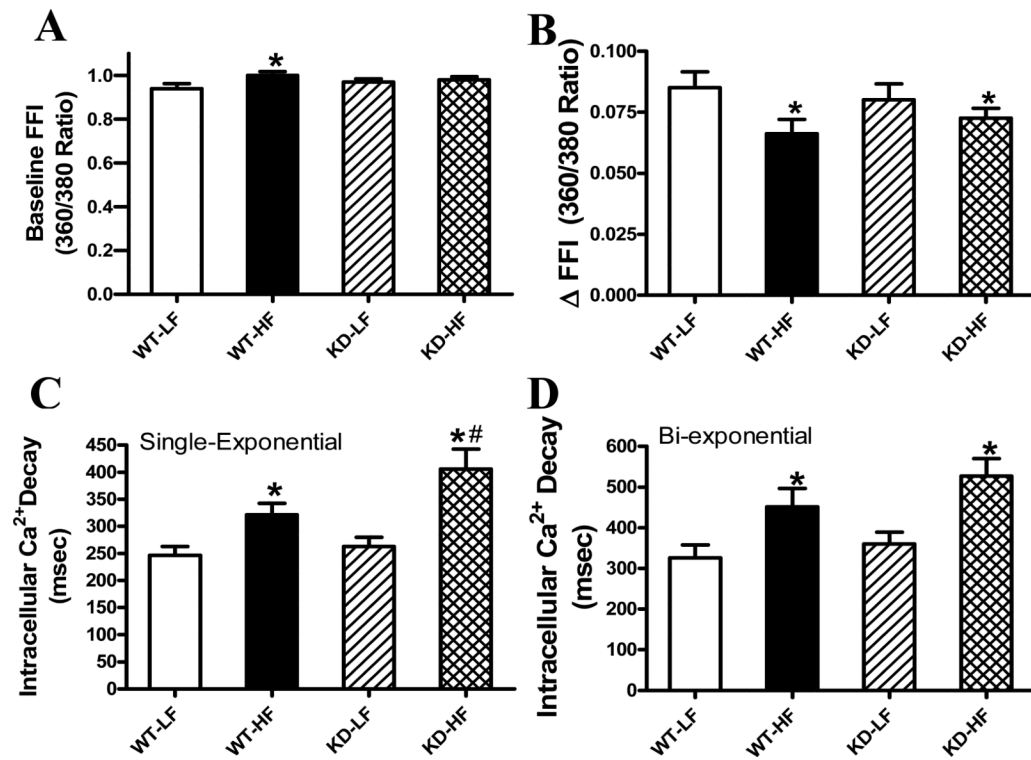
**Fig 4.**
Intracellular $Ca^{2+}$ transient properties in cardiomyocytes from low fat (LF) and high fat (HF)-fed WT and AMPK KD mouse hearts. A: Resting fura-2 fluorescence intensity (FFI); B: Electrically-stimulated rise in FFI ( FFI); C: Single exponential intracellular $Ca^{2+}$ decay rate; and D: Bi-exponential intracellular $Ca^{2+}$ decay rate. Mean ± SEM, n = 50 cells per group from 4-5 mice, * $p < 0.05$ *vs.* WT-LF group, # $p < 0.05$ *vs.* WT-HF group.
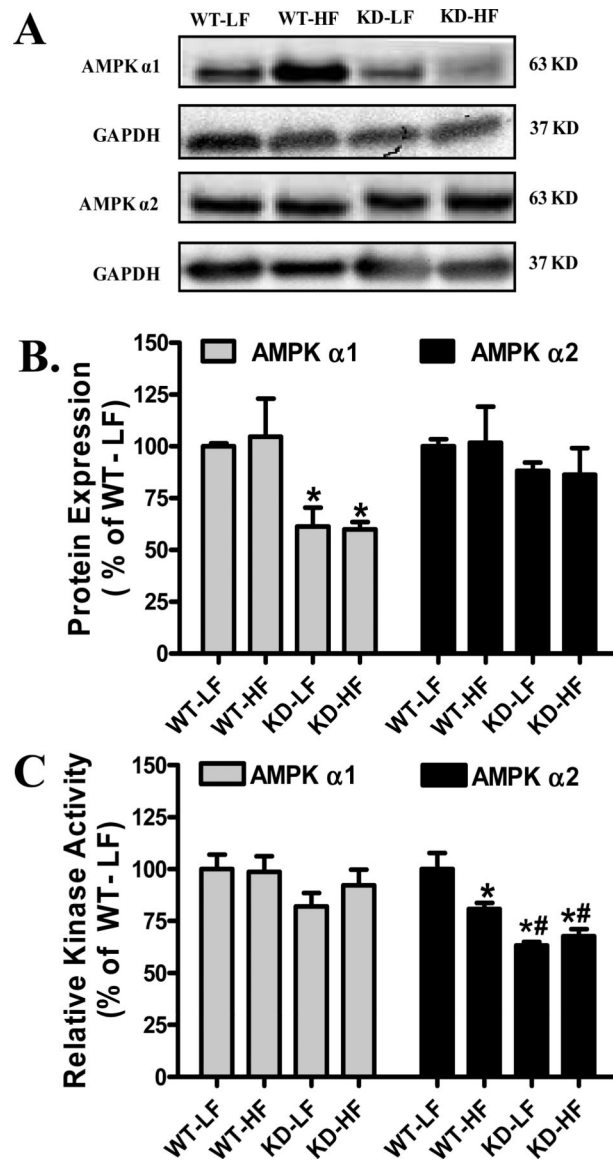
**Fig. 5.**
Protein expression and activity of AMPK α isoforms in left ventricular protein lysates from low fat (LF) and high fat (HF)-fed WT and AMPK KD mice. A: Representative gel blots depicting AMPKα1, AMPKα2 and GAPDH (loading control) using specific antibodies; B: Protein expression of AMPKα1 and AMPKα2; and C: Isoform-specific AMPK activity in left ventricular protein lysates from LF and HF-fed WT and AMPK KD mice. Mean ± SEM, n = 6-8, * $p < 0.05$ *vs.* WT-LF group, # $p < 0.05$ *vs.* WT-HF group.
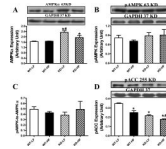
**Fig. 6.**
AMPK expression as well as activation of AMPK and ACC in myocardium from low fat (LF) and high fat (HF)-fed WT and AMPK KD mice. A: AMPKα; B: pAMPK; C: pAMPK/AMPK ratio; and D: pACC. Inset: Representative gel blots depicting AMPKα, pAMPK, pACC and GAPDH (loading control) using specific antibodies. Mean ± SEM, n = 4, * p < 0.05 *vs.* WT-LF group, # p < 0.05 *vs.* WT-HF group.
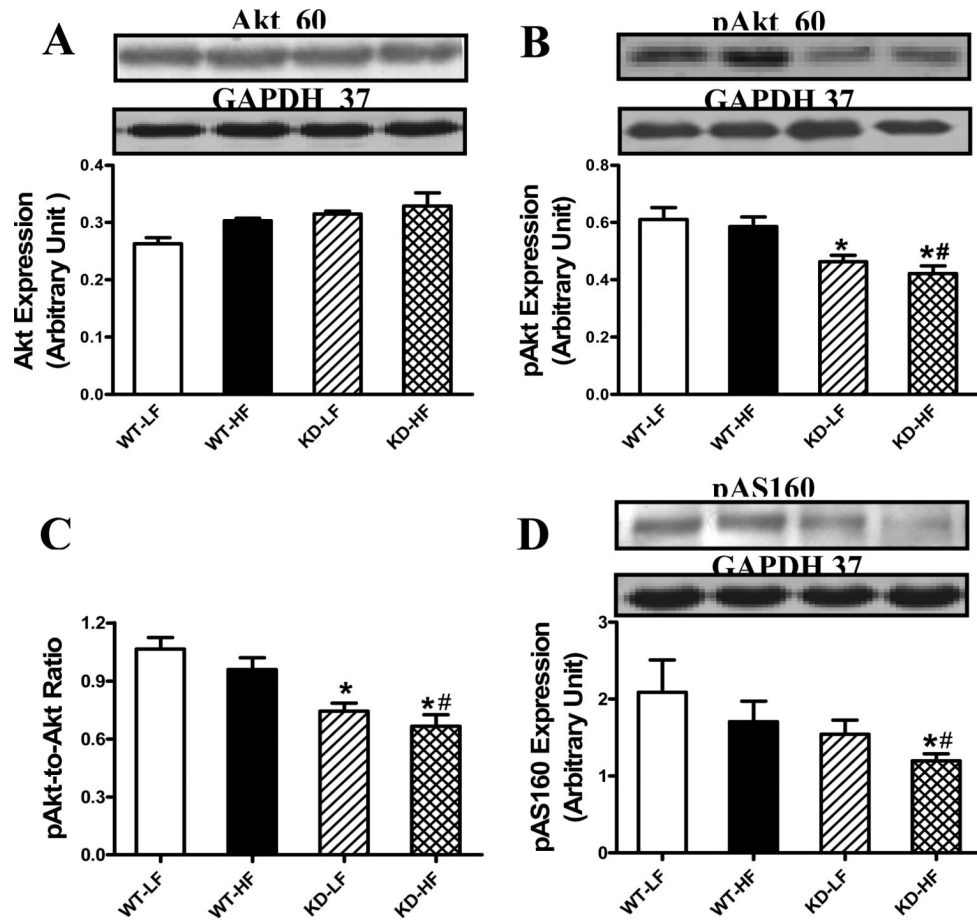
**Fig. 7.**
Protein expression of Akt, pAkt and pAS160 in myocardium from low fat (LF) and high fat (HF)-fed WT and AMPK KD mice. A: Akt; B: pAkt; C: pAkt/Akt ratio; and D: pAS160. Inset: Representative gel blots depicting Akt, pAkt, pAS160 and GAPDH (loading control) using specific antibodies. Mean ± SEM, n = 4, * p < 0.05 *vs.* WT-LF group, # p < 0.05 *vs.* WT-HF group.
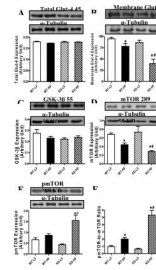
**Fig. 8.**
Protein expression of Glut-4, GSK-3β and mTOR in myocardium from low fat (LF) and high fat (HF)-fed WT and AMPK KD mice. A: Total Glut-4; B: Membrane fraction of Glut-4; C: GSK-3β; D: mTOR; E: phosphorylated mTOR (pmTOR) and F: pmTOR/mTOR ratio. Inset: Representative gel blots depicting total Glut-4, membrane GLUT4, GSK-3β, mTOR and pmTOR. Mean ± SEM, n = 4-5 per group, * p <0.05 vs. WT-LF group, # p < 0.05 *vs.* WT-HF group.

**Table 1**

Biometric parameters of WT and AMPK KD mice with low fat (LF) or high fat (HF) diet for 20 weeks.

| | WT-LF | WT-HF | KD-LF | KD-HF |
|---|---|---|---|---|
| Body Weight (BW, g) | 26.2 ± 1.0 | 33.7 ± 0.8* | 26.5 ± 0.6 | 33.6 ± 0.7* |
| Heart Weight (HW, mg) | 131 ± 4 | 168 ± 5* | 147 ± 10 | 195 ± 8*,# |
| HW/TL (mg/mm) | 7.68 ± 0.20 | 9.56 ± 0.49* | 8.36 ± 0.29 | 10.95 ± 0.43*,# |
| Liver Weight (LW, g) | 1.38 ± 0.04 | 1.59 ± 0.03* | 1.43 ± 0.05 | 1.70 ± 0.10* |
| LW/BW (mg/g) | 53.6 ± 1.94 | 48.1 ± 1.6 | 54.6 ± 2.8 | 50.4 ± 2.6 |
| Kidney Weight (KW, g) | 0.37 ± 0.02 | 0.48 ± 0.02* | 0.44 ± 0.01 | 0.52 ± 0.02* |
| KW/BW (mg/g) | 13.9 ± 0.6 | 14.4 ± 0.7 | 16.7 ± 0.5 | 14.8 ± 0.4 |
| Body Fat Composition (%) | 28.0 ± 1.6 | 48.4 ± 5.8* | 22.5 ± 2.0 | 46.5 ± 4.7* |
| Plasma Insulin (ng/ml) | 0.44 ± 0.09 | 0.90 ± 0.09* | 0.44 ± 0.08 | 1.01 ± 0.35* |
| Heart Rate (bpm) | 452 ± 30 | 465 ± 11 | 519 ± 18 | 505 ± 36 |
| Wall thickness (mm) | 0.77 ± 0.10 | 0.88 ± 0.03 | 0.74 ± 0.08 | 0.87 ± 0.06 |
| EDD (mm) | 2.09 ± 0.09 | 2.51 ± 0.16* | 2.29 ± 0.28 | 3.40 ± 0.31*,# |
| ESD (mm) | 0.89 ± 0.11 | 1.64 ± 0.17* | 1.11 ± 0.11 | 2.14 ± 0.19*,# |
| LV mass (mg) | 49.6 ± 4.9 | 77.7 ± 9.3* | 43.4 ± 5.0 | 85.9 ± 10.6* |
| Normalized LV mass (mg/g) | 1.91 ± 0.16 | 2.37 ± 0.22* | 1.84 ± 0.20 | 2.53 ± 0.37* |
| Fractional Shortening (%) | 48.8 ± 1.8 | 35.9 ± 3.4* | 47.3 ± 1.3 | 27.4 ± 1.0*,# |
| Diastolic blood pressure | 83.1 ± 4.3 | 87.2 ± 6.1 | 83.1 ± 8.1 | 85.5 ± 5.8 |
| Systolic blood pressure | 111.1 ± 6.1 | 119.0 ± 4.6 | 118.2 ± 3.2 | 121.3 ± 6.6 |

Tibial length: TL; EDD: end diastolic diameter; ESD: end systolic diameter; Left ventricular: LV. Mean ± SEM

For echocardiography and blood pressure analysis, n = 8; all other parameters: n=13 -15 mice per group.

*
p < 0.05 *vs.* WT-LF group

#
p < 0.05 *vs.* WT-HF group.